Buckling behaviour of PPS/CF laminates stiffened by induction welding

Gennaro Scarselli[1], Silvio Pappadà[2], Giuseppe Buccoliero[2],
Andrea Salomi[2], Alfonso Maffezzoli[1]

[1] University of Salento, Department of Engineering for Innovation, Via per Monteroni, 73100 Lecce, Italy.
[2] Consorzio CETMA, Departments of Materials and Structures Engineering, Technologies and Processes Area, SS7 – Km 706+300, 72100 Brindisi, Italy.

Abstract
Thermoplastic materials are getting increasing attention in the aerospace field for a wide range of applications not only related to primary structures. In this work two types of thermoplastic structures are manufactured and investigated: a L-shaped stringer used as stiffener of flat plates; a stiffened panel for aerospace applications. The panel has been reinforced using four L-shaped stringers joined to it by induction welding, an innovative technique alternative to mechanical fastening and adhesive bonding. The main focus of this work is experimentally demonstrating the capability of the welding to keep properly the loads arising from a compression test until the failure of the stiffened panel. Interesting results came out concerning the post-buckling behaviour of the adopted thermoplastic materials that exhibited outstanding load bearing capabilities.

Introduction

The aircraft structures should be light and resistant, able to operate efficiently with the minimum weight and with proper margins of safety. In the last twenty years a rapid growth in the employment of composites as structural materials in the aerospace field occurred. At first the attention was focused on thermoset-matrix based composites. The attention is now devised towards materials involving a thermoplastic matrix. This because thermoplastic composites have higher damage tolerance and interlaminar toughness, as well as many other advantages, such as recyclability after life-cycle, reprocessing, faster production processes, chemical and environmental resistance, reduced moisture absorption, longer shelf life over the thermoset ones. The automotive industry has traditionally produced a wide range of thermoplastic parts with the advantage of shorter processing times and fully automated equipment [1, 2, 3]. In the late 1980s, glass and carbon reinforced hermoplastic matrix laminates were first used in Fokker 100, Gulfstream G400 and G500 business ets, and Airbus Beluga transport aircraft as thermoformed flooring panels [4, 5]. More recently, hermoplastic composites have found application in landing gear doors, winglets, elevators, ilerons, flaps, spoilers, speed brakes, slats and so on [6, 7, 8]. A wide range of high thermoplastic natrices is available nowadays, with PEEK and PPS the most studied and reported.
oining plays an important role in manufacturing of composite structures in marine, automotive and erospace industry. Mechanical fastening and adhesive bonding are widely used to assemble metals r composite components. However, there are some disadvantages associated with these methods: rilling operations induce stress concentration around the holes and adhesive bonding requires an ccurate surface preparation and long curing times. The joints of thermoplastic matrix composites an be realized using various welding methods such as electric resistance, ultrasonic, vibration, hot late, electromagnetic induction, dielectric/microwave and IR welding [9, 10, 11]. As reported by a Costa et al [12] it is not possible to identify one welding technique suitable for all the different ndustrial situations: all the techniques show advantages and drawbacks and they may be more or ess suitable to a particular application depending on its specific requirements. Among the various echniques of this category, the most mature ones seem the ultrasonic, induction and resistance welding. Most of the primary structures of aircrafts are essentially made of a box able to withstand

Excerpt from ISBN 978-3-00-053387-7

torsion, shear and bending. The flexural behaviour of box like structures made with stiffened plates involves significant compressive stresses that can lead to the buckling, global or local, of the different structural components of the wing box. Co-curing and co-bonding are often used with thermosetting matrix composites when adhesion bonding is adopted to join the stringers to the plate, even if bolted joints are still the most used solution [13].
In this work the buckling behaviour under compression of a composite laminate made using Poly Phenilene Sulfide (PPS) as matrix and a carbon fiber fabric as reinforcement was studied. The composite laminate was stiffened by four L-shaped stringers bonded by induction welding. Compression tests were performed also on the L stringers. The obtained results coupled with mechanical testing on small specimens were used to assess the mechanical properties of the composite. During the buckling tests of the L-shaped stringers, the load was increased above the critical load highlighting an impressive ductility of the thermoplastic material and the strong capability of bearing further loads well beyond the first critical threshold. This outstanding residual strength of the thermoplastics, under post-buckling conditions, makes them definitely suitable for the primary aircraft structure since, under axial compression, even if a structural member does buckle, the design can have sufficient load-carrying capacity to survive up to ultimate load. In addition, the buckling tests revealed that the final break of the stiffened panel did not involve the induction welded interfaces. Visible damages affected several stringers failed under compression. Finite Element (FE) analysis in linear and non linear conditions was performed using MSC Nastran. Shell elements were used to simulate stringers and panel and the induction welded interface was simulated by rigid connection of the nodes belonging to stringers and panel. The first static, linear and non-linear, simulations were aimed at calibrating the numerical model based on the actual material properties. Geometric non-linearities have been then taken into account to simulate the structural behaviour when large displacements occur before and after the buckling. The buckling and the post-buckling conditions of the stringer and of the stiffened panel were simulated achieving a good match between experimental and numerical data.

Materials and methods

Two types of structures have been tested: a L-shaped stringer commonly used as stiffener of flat panel and a stiffened panel. Buckling loads have been experimentally evaluated and, in parallel, numerical simulations have been carried out in order to have a reliable mathematical model of the structures suitable for analyses of conditions different from the tested ones. Small coupons have been manufactured with the same properties of the stringer and the panel to be tested in order to obtain the material mechanical properties.
The stiffened panel was obtained using a carbon-fibre fabric reinforced polyphenylensulfide (PPS), ıe CETEX® composite laminate provided by TENCATE (5-harness satin; fibre volume fraction: 0%). A 500x500 mm flat laminate, characterized by a thickness of 1.2 mm, was used as base plate lay-up: [±45/0/90/0/90/±45]) stiffened by four L-shaped stringers, obtained by match die moulding :om 1.8 mm thick laminates (lay-up: $[0/90/0/90/0/90]_S$). The L-shaped stringer was 400 mm long. he specimens are sketched in Figure 1 and Figure 2.
he welding of the stringers to the panel was performed with a 600 kHz, 220 V induction generator, esigned and developed by Cetma and Sinergo (Italy). The stiffeners were welded using a double-D" coil, a welding speed of 2 mm/s, a coil distance from the surface of 2 mm and a power f 1.25 kW at a frequency of 600 kHz and a tension of 220 V. The fabrication of the prototype and rocess modelling has been reported in a former paper [14]. In the induction welding set-up (Figure), heating is produced within the conductive carbon fibre meshes present in the composite fabric, nd the temperature in the welding region is increased above the melting temperature of PPS matrix p to 340 °C, while the temperature of the upper surface of the joining is kept below 220 °C, thanks o an air flow, and a continuous control through an optical pyrometer.

Excerpt from ISBN 978-3-00-053387-7

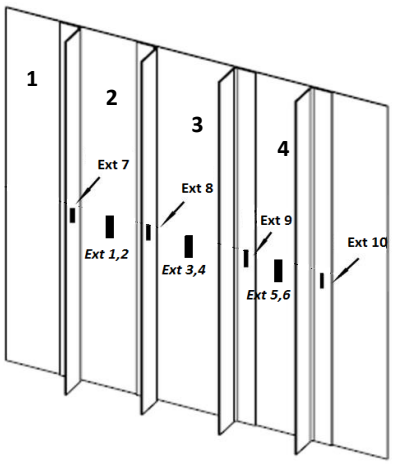

Figure 1: stiffened panel equipped with strain gauges (the stringers are numbered from left to right)

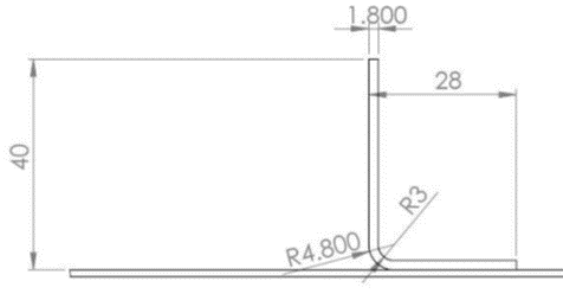

Figure 2: L-shaped stringer geometry (flange 1 is the horizontal one; flange 2 is the vertical one)

A cooled roller applies the consolidation pressure and rapidly cools the molten material below its crystallization temperature. Buckling and post-buckling behaviour of the stringer has been characterized performing compression tests with a dynamometer MTS 100. Four strain gauges were used during stringer compression test and ten for the stiffened panel (see Figure 1). The out-of-plane displacement of the flat panel was monitored using two LVDT.

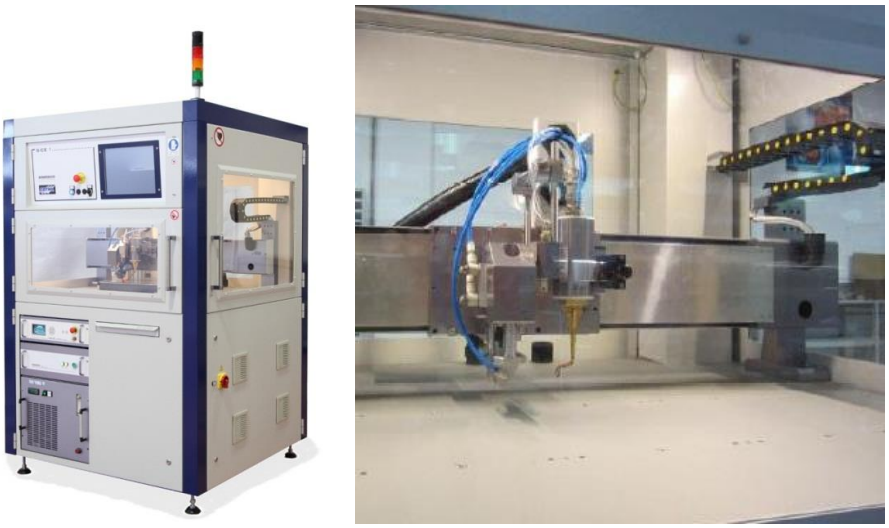

Figure 3: view of the induction welding machine (on the left) and detail of the welding head (on the right)

Excerpt from ISBN 978-3-00-053387-7

Experiments

Stringer

As shown in Figure 4 the stringer was connected at the ends of custom made L-shaped tools and two strain gauges have been mounted on each of the two flanges of the stringer in order to evaluate the deformations. The load-displacement curve related to the buckling test of the stringer is reported in Figure 5.

The main results come out from the experimental tests were the following: a first buckling load appeared at 650 N followed by a very long flat region in which the load was almost constant and the stringer kept on deforming; afterwards the stringer assumed a different geometric configuration and exhibited again the attitude to take incremental loads. This resulted in an outstanding post-buckling behaviour until a new catastrophic buckling load appeared at 8000 N. Immediately after this new threshold was exceeded, the stringer failed showing visible fibers breakage at the mid span and the test was interrupted (see Figure 6).

Figure 4: buckling test set-up for the stringer

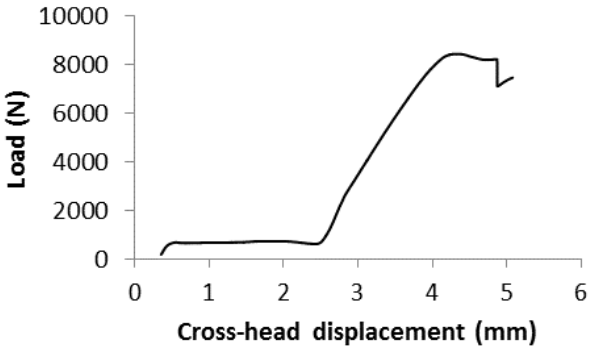

Figure 5: load – displacement curve in a compression test performed on the stringer

Figure 6: the stringer after the buckling test

Stiffened panel

Buckling and post-buckling behaviour of the stiffened panel has been investigated performing compression tests. The compression load was simultaneously applied at the edges of the base panel and stringers as shown in Figure 7.

The main result of the experimental tests has been that the panel-to-stringers welded joints withstood properly the compressive load throughout all the test. No damage or debonding appeared in the contact area between any stringer and the panel even after the completion of the buckling test, after all the four stringers were visibly damaged. The first buckling appeared at 10.2 kN; afterwards the panel was able to withstand further incremental loads.

As shown in Figure 8 the following typical features of a buckling test occurred: the nonlinear structural behaviour resulting in a nonlinear load-displacement curve due essentially to large deformations; the sudden decreases of load due to several fibres breakage inside the panel; the flat regions due to the transition at the buckling load from a stable geometric configuration to another one without incremental load.

The failure of the panel involved essentially the stringers that, under the action of the compressive load that becomes eccentric for the big deformations, bent until the rupture occurs. Research activities are planned in the near future aimed at monitoring the welded interface by advanced non-linear methods of damage detection [15].

Excerpt from ISBN 978-3-00-053387-7

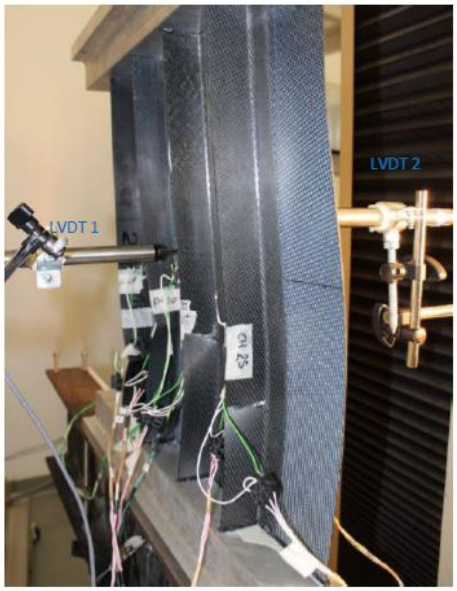

Figure 7: buckling test set-up for the panel

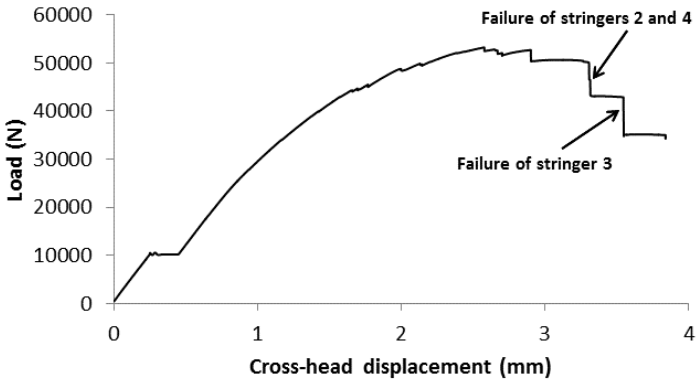

Figure 8: load – displacement curve from the test

Characterization of the materials

From the same manufacturing set, samples of stringer and panel were produced to perform structural tests aimed at the characterization of the materials. From Figure 9 to Figure 12, the samples for the materials characterization are represented together with the corresponding stress-strain curves and elastic moduli.

Figure 9: stringer sample

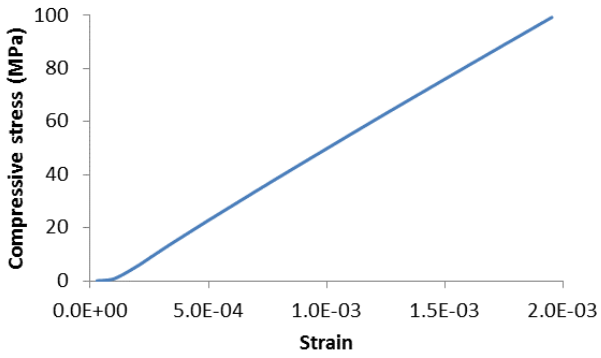

Figure 10: test on the stringer sample

$E_{x,exp}$ = 53.0 GPa
$E_{x,nom}$ = 54.5 GPa

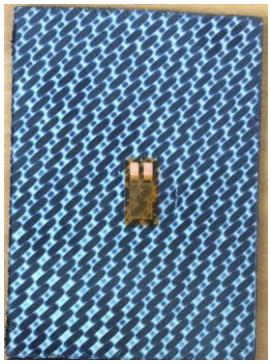

Figure 11: panel sample

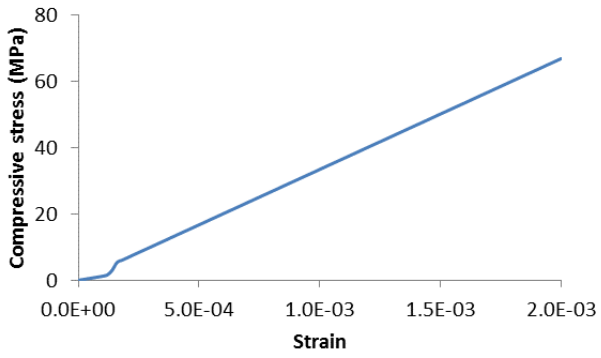

Figure 12: test on the panel sample

$E_{x,exp}$ = 35.9 GPa
$E_{x,nom}$ = 33.0 GPa

The found experimental values for the Young's moduli ($E_{x,exp}$) of the two materials were very close to the nominal values calculated combining the classical micro- and macro-mechanical analysis of the composite laminates ($E_{x,nom}$). The experimental values were adopted for the Finite Element

Excerpt from ISBN 978-3-00-053387-7

Analyses (FEA) of the stringer and the stiffened panel under the action of compressive load and constrained as for the tests.

Numerical Analysis, results and discussions

FEA were carried out on the stringer and the stiffened panel using Patran/Nastran commercial software. SOL105 (Linear Buckling Analysis) was performed in order to evaluate the first buckling loads and modes. CQUAD4 elements of the Nastran library were used for simulating the structure. In a first model, the constraints of the stringer at each end were fixed supports to reproduce the boundary conditions during the test (see Figure 13).

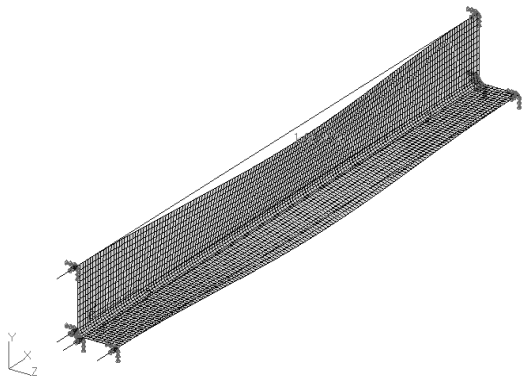

Figure 13: first buckling mode of the stringer in linear analysis

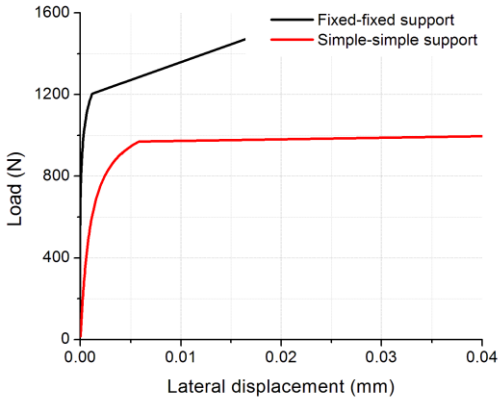

Figure 14: nonlinear static analyses of the stringer: load-lateral deflection curve

The first three buckling loads provided by the linear numerical analyses were 1.2 kN, 2.00 kN and 3.16 kN. Nonlinear static analyses (SOL106), taking into account the big deformations of the structure under the action of compressive load, were performed in order to reproduce the test and to evaluate the buckling and post-buckling behaviour of the stringer. Two different boundary conditions were simulated, simple supports and fixed support at the edges. As shown in Figure 14 it is clear that this type of analysis (SOL106) provides similar results to the linear buckling analysis (SOL105): the lateral displacement represents the displacement normal to the stringer longitudinal axis that diverges at the buckling load as expected. The calculated first buckling load was 1.2 kN, about the double of the measured one, i.e. 0.65 kN. Also the improper description of the boundary conditions was not a possible explanation of this poor agreement between the numerical analysis and the experiments. Indeed the fixed support constraints at the ends of a beam are not easy to achieve in laboratory but also using hinges (simple supports) the first buckling load decreased at 1.80 N, not enough to match the experimental value (see Figure 14). Therefore it was assumed that a local instability, typical of the aeronautical structures made of assembled thin-walled beams, could be responsible of the lower experimental buckling load. Two types of structural instability are possible, a global one, involving the beam as a whole (the buckle length is of the same order of magnitude of the beam length) and a local one involving sub-elements of the structure (the buckle length is of the same order of magnitude of the typical section dimensions). Local instability analysis is usually performed focusing the attention on the sub-elements of the structure which in this case are represented by the two flanges of the L-shaped stringer. A separate analysis of their buckling behaviour with fixed constraints at the ends and hinges at the nodes placed at the mutual interface has been performed. The buckling loads found were 0.87 kN for the instability of the flange 1 of the stringer (see Figure 2) and 0.69 kN for the instability of the flange 2: this meant that the flange 2 buckled under the action of a compressive load of 0.69 kN applied to the whole section of the stringer, a value very close to 0.65 kN experimentally found. This result confirmed that the investigated structural component suffered a local instability.

Excerpt from ISBN 978-3-00-053387-7

The numerical model of the stiffened panel was developed in order to have a reliable structural model suitable for simulations of conditions different from the tests.

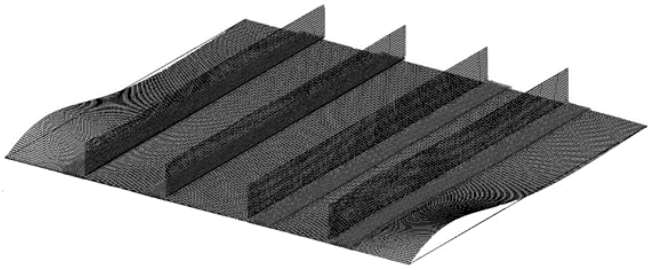

Figure 15: the first buckling mode of the stiffened plate

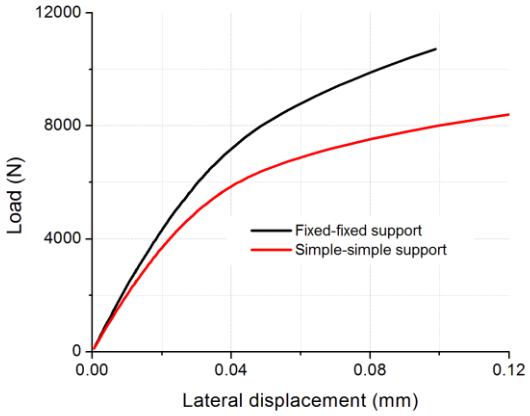

Figure 16: nonlinear static analyses of the stiffened panel

CQUAD4 elements were used also in this case both for the stringers and the flat panel. The joint of the stiffeners to the panel was simulated simply merging the interface nodes between the two parts. According to the experiments, the two edges were subjected to a compressive load applied by a pressure distributed on the sides of the CQUAD4 elements. The other two edges were unloaded and free. The first three buckling loads found numerically by the SOL105 were: 11.7 kN, 11.8 kN and 12.5 kN and the first buckling mode involved displacements of the free edges as expected (see Figure 15). The nonlinear static analysis of the stiffened panel in this case (see Figure 16) did not provide a clear divergence at the buckling load of the lateral deflection in the middle of the panel as in the case of the stringer. The numerical results provided by the SOL105, anyway, were in a very good agreement with the experimental ones (the first experimental buckling load was 10.2 kN close to the numerical value of 11.7 kN). A possible modification of the stiffened panel was conceived in order to increase the buckling load without complicating too much the design and its manufacturing. An alternative geometry was conceived for the stringer changing the section from L shape to C shape. The numerical results of the simulation related to this modified panel are reported in Table 1.

	L-shaped stringer	C-shaped stringer	Variation
Panel weight	680 g	803 g	+18%
Buckling load	11700 N	19500 N	+67%

Table 1: effect of section shape modification of the stringer

The proposed modification of the stringer led to a percent increase of weight for the panel of 18% to which corresponded an increase of buckling load of 67%. In the aeronautical field modifications leading to weight increase are strongly undesired. Nevertheless these results gave a clear idea of how sensitive was the buckling load to the stiffener shape.

Conclusions

The present work was focused on buckling and post-buckling behaviour of thermoplastic composites for aerospace application. Furthermore a demonstration of the effectiveness of induction welding as joining technique until the ultimate load on typical aerospace panels was provided. Two structural components were tested: one L-shaped thermoplastic stringer; one flat panel reinforced with four of these L-shaped stringers bonded by induction welding. Experimental activities were aimed at the characterization of the adopted materials and the evaluation of buckling loads of the tested structures. The L-shaped stringer showed an outstanding structural behaviour being able to

Excerpt from ISBN 978-3-00-053387-7

take huge loads after the first buckling appeared. The tests on the stiffened panel demonstrated that induction welding is effective until the structural ultimate load and no debonding areas were visible at the interface between the stringers and the panel. The numerical activities provided, indeed, results in good agreement with the experimental ones, taking into account either the geometric nonlinearities associated with the big deformations of the structures under the action of compressive loads either the buckling of the flanges composing the stringer.

References

1. Ray, B. C."Temperature effect during humid ageing on interfaces of glass and carbon fibers reinforced epoxy composites.", Journal of Colloid and Interface Science 298.1 (2006): 111-117.
2. Botelho, E. C., et al. "Processing and hygrothermal effects on viscoelastic behavior of glass fiber/epoxy composites.", Journal of Materials Science 40.14 (2005): 3615-3623.
3. Todo, Mitsugu, et al. "Strain-rate dependence of the tensile fracture behaviour of woven-cloth reinforced polyamide composites.", Composites Science and Technology 60.5 (2000): 763-771.
4. Vieille, Benoit, Jérémie Aucher, and Lakhdar Taleb "Influence of temperature on the behavior of carbon fiber fabrics reinforced PPS laminates.", Materials Science and Engineering: A 517.1 (2009): 51-60.
5. Botelho, E. C., M. C. Rezende, and B. Lauke "Mechanical behavior of carbon fiber reinforced polyamide composites.", Composites Science and Technology 63.13 (2003): 1843-1855.
6. De Faria, M. C. M., et al. "The effect of the ocean water immersion and UV ageing on the dynamic mechanical properties of the PPS/glass fiber composites." Journal of Reinforced Plastics and Composites 30.20 (2011): 1729-1737.
7. Bates, P. J., et al. "Shear strength and meltdown behavior of reinforced polypropylene assemblies made by resistance welding" Composites Part A: Applied Science and Manufacturing 40.1 (2009): 28-35.
8. Arici, Aziz Armagan. "Effect of hygrothermal aging on polyetherimide composites." Journal of Reinforced Plastics and Composites 26.18 (2007): 1937-1942.
9. Mouzakis, Dionysis E., Helen Zoga, and Costas Galiotis. "Accelerated environmental ageing study of polyester/glass fiber reinforced composites (GFRPCs)." Composites Part B: Engineering 39.3 (2008): 467-475.
10. Wang, Ying, and Thomas H. Hahn. "AFM characterization of the interfacial properties of carbon fiber reinforced polymer composites subjected to hygrothermal treatments." Composites science and technology 67.1 (2007): 92-101.
11. Loos, Alfred C., et al. "Moisture absorption of polyester-E glass composites." Journal of Composite Materials 14.2 (1980): 142-154.
12. da Costa, Anahi Pereira, et al. "A Review of welding technologies for thermoplastic composites in aerospace applications" doi 10.5028/jatm. 2012.040303912, Journal of Aerospace Technology and Management 4.3 (2012): 255-266.
13. Scarselli, G., et al. "Structural behaviour modelling of bolted joints in composite laminates subjected to cyclic loading." Aerospace Science and Technology 43 (2015): 89-95.
14. Silvio Pappadà, Andrea Salomi, Jeanette Montanaro, Alessandra Passaro, Antonio Caruso, Alfonso Maffezzoli, "Fabrication of a thermoplastic matrix composite stiffened panel by induction welding" Aerospace Science and Technology, Volume 43, (2015), Pages 314-320, doi: 10.1016/j.ast.2015.03.013.
15. Ciampa, Francesco, Gennaro Scarselli, and Michele Meo "Nonlinear imaging method using second order phase symmetry analysis and inverse filtering." Journal of Nondestructive Evaluation 34.2 (2015): 1-6.

Excerpt from ISBN 978-3-00-053387-7